Supporting Information

Drazic et al. 10.1073/pnas.1300578110

SI Experimental Procedures

Data Presentation. Values are given either as a result from one representative experiment or as mean ± SD ($n \geq 3$).

Generation of Mutants. Deletion strains were generated using the method by Datsenko and Wanner (1) and confirmed by PCR amplification of the deleted region. Strain KMG232 was generated by deleting the chloramphenicol cassette in the hypochlorite-responsive transcription factor (*hypT*) gene according to ref. 1. HypT mutants were generated in the plasmids pET11a (Novagen) and pBAD22 [pJW2 (2)] by site-directed mutagenesis. Flash-tagged mutants were generated using the primer forward *yjiE* and reverse *yjiE*-flash (3) and cloning the NdeI/HindIII-digested PCR fragment into pET28a [pAD2 (3)]. A list of strains used in this study can be found in Table S1.

Cultivation of Strains. Strains were cultivated in LB medium with the appropriate antibiotics. Expression of *hypT* or mutants for purification purposes was performed in BL21(DE3) cells using isopropyl-ß-D-thiogalactopyranosid (IPTG) (0.1 mM). Cultures of the various C600 cells were cultivated overnight and then diluted 1:100, and arabinose [0.1% (wt/vol)] was added immediately unless indicated otherwise. Cells were cultivated until an OD_{600} of 0.45–0.5 was reached. Then, cultures were used for viability assays, quantitative qRT-PCR, or Western blot analysis.

Western Blot Analysis. Cells were cultivated as described above (± stress treatment), samples were removed, and cell pellets were resuspended in reducing sample buffer. Proteins were separated on a neutral gel (SERVA) and blotted onto PVDF membrane followed by decoration with HypT-specific or methionine sulfoxide reductase (Msr)B-specific antibodies as indicated. Protein bands were quantified using ImageJ software (National Institutes of Health). Induction of *hypT* expression with 0.1% arabinose (2.5 h) yielded about 200 ng HypT per 1 mL cells with OD 1, corresponding to about 20 times the wild-type level.

Viability Assays. Viability assays using C600 cells in LB medium were performed as described with hypochlorite (HOCl) (3.5 mM final concentration) or H_2O_2 (2 mM) (3). Please note that HOCl reacts with LB medium components, thus requiring millimolar concentrations of HOCl for efficient killing.

Quantitative Real-Time PCR. qRT-PCR and sample preparation of HOCl-stressed samples were performed as described (3) with the exception that 10 mL cells was cultivated and 1-mL samples were harvested by centrifugation for 1.5 min (4 °C, 17,000 × *g*). Viability of cells during the time course of the experiment was 100%. Elongation factor TU (TufB) RNA was used as an endogenous control to normalize the variation of RNA template in each sample. RNA levels of the untreated control sample were set to 1. As a control, HOCl-treated cells were analyzed for viability (see above). Viability of cells was always 100%.

For recovery experiments, YLe143, KMG229, HM16, and HM17 cells were cultivated in 10 mL LB medium containing arabinose [0.1% (wt/vol) final concentration] and ampicillin until an OD of 0.45 was reached. Then, 10 mL cells was supplemented with HOCl (2.75 mM, 10 min) and afterward 2 mL fivefold concentrated LB medium was added to quench HOCl and allow recovery of the cells. Samples were removed before, during, after the stress. Samples were harvested (1.5 min, 4 °C, 17,000 × *g*), the supernatant was completely removed, pellets were frozen in liquid nitrogen, RNA was isolated, and qRT-PCR was performed as described (3). If applicable, the decrease in RNA levels was fitted using a single exponential function. The time constant ($t = 1/e$) was determined and is given in minutes.

For the analysis of constitutive activity, YLe143, KMG229, JW458, and JW477 cells were cultivated in LB medium supplemented with ampicillin until an OD_{600} of 0.45 was reached. Then, arabinose [0.1% (wt/vol)] was added to induce expression of the desired mutant gene. No HOCl was added. Samples were removed at various time points and prepared as described above.

Protein Purification and Analysis of DNA Binding. Expression of *hypT* from a pET11a plasmid was performed in BL21(DE3) cells by induction with 0.1 mM IPTG (yielding about 1–3 μg soluble HypT per 1 mL cells with OD 1). Purification of proteins, either unstressed or HOCl-stressed (final concentration 2–3 mM HOCl), was performed as described (3). Proteins contained a C-terminal His tag, which does not change structural characteristics and does not influence the function of HypT, as demonstrated (3).

Analysis of DNA binding was performed by fluorescence anisotropy (FA) using Alexa Fluor 488–158-bp *metN*-promoter or Alexa Fluor 488–158-bp *hypT*-promoter DNA and unlabeled HypT variants exactly as described (3). Protein (2 μM) was added to 10 nM DNA. Fluorescence anisotropy (*r*) values are given.

In Vitro Activation of HypT. Cysteines in purified HypT were glutathionylated (1 mM oxidized glutathione, 1 h, 37 °C), and samples were desalted using an NAP5 column (GE Healthcare) and buffer (10 mM NaH_2PO_4, 400 mM NaCl, pH 7.5). Then, samples were incubated with HOCl at a molar ratio of HOCl to HypT of 4:1, 5:1, 6:1, and 7:1 (1 h, 37 °C). Samples were desalted and concentrated using a 10K Centricon tube (Millipore). Glutathionylated protein samples were then reduced with DTT (3 mM, 2 h, 37 °C) before further analysis.

Proteolytic Digest for Mass Spectrometric Analyses. For the analysis of oxidative modifications and their localization on HypT, purified protein was denatured (4 M urea, 37 °C, 2 h) and reduced [1 mM tris(2-carboxyethyl)phosphine (TCEP)] unless indicated otherwise, fivefold diluted in digest buffer, and incubated with the respective protease(s) under nitrogen atmosphere for at least 24 h. Trypsin digests (T; mass ratio of 1:100) were performed in 50 mM Tris·HCl (pH 7.5), 1 mM $CaCl_2$ at 37 °C. Combined trypsin and chymotrypsin digests (T + C; mass ratios of 1:100 and 1:20, respectively) were carried out in 50 mM ammonium bicarbonate (pH 7.8), 1 mM $CaCl_2$ at 25 °C. Combined trypsin and Glu-C digests (T + G; mass ratios of 1:100 and 1:20, respectively) were carried out in 25 mM ammonium bicarbonate (pH 7.8), 1 mM $CaCl_2$ at 25 °C.

The following digests were performed: (*i*) HypT from wild-type cells: unstressed [T ($n = 4$), T + C ($n = 7$), T + G ($n = 1$)], HOCl-stressed [T ($n = 1$), T + C ($n = 4$), T + G ($n = 1$)], after 15-min recovery [T ($n = 2$), T + C ($n = 3$), T + G ($n = 1$)]; (*ii*) in vitro activated HypT: [T ($n = 6$), T + C ($n = 6$)]; (*iii*) HypT from $msrA^-$ $msrB^-$ cells: unstressed [T ($n = 1$), T + C ($n = 2$), T + G ($n = 1$)], HOCl-stressed [T ($n = 3$), T + C ($n = 4$), T + G ($n = 1$)], after 15-min recovery [T ($n = 3$), T + C ($n = 4$), T + G ($n = 1$)]; and (*iv*) in vitro treated HypT-$HOCl^{2.75\ mM}$: +DTT [T ($n = 2$), T + C ($n = 3$), T + G ($n = 1$)], +MsrA/MsrB [T ($n = 2$), T + C ($n = 2$)], + DTT +MsrA/MsrB [T ($n = 5$), T + C ($n = 9$), T + G ($n = 2$)].

Mass Spectrometric Analyses. Digested samples were precleared by filtration through a 0.22-μm centrifuge filter (Millipore) before

subjection to a nano liquid chromatography system (Ultimate 3000; Thermo Scientific) coupled online to an Orbitrap XL mass spectrometer (Thermo Scientific). Peptides were loaded on an Acclaim PepMap RSLC C18 trap column (75 μm × 150 mm, C18, 2 μm, 100 Å; Thermo Scientific), desalted, concentrated, and then separated by applying a linear gradient from 5% to 35% buffer B (100% acetonitrile with 0.1% formic acid) in 30 min. Full-scan spectra of multiply charged ions were recorded in the Orbitrap cell with a resolution of 60,000 at *m/z* 400. Per cycle, six dependent MS/MS scans of the three most intense ions of each full scan were measured, comprising three collision-induced dissociation (CID) and three higher energy collisional dissociation (HCD) fragmentation spectra.

Raw files were processed using the SEQUEST algorithm implemented in Proteome Discoverer 1.3 (Thermo Scientific) with a database containing HypT sequences (including affinity tags) with the following parameters: three missed cleavage sites, search tolerance 10 ppm, and 0.8 Da for precursor and MS2 spectra. To obtain good sequence coverage for each sample, results from different digestion reactions of identical samples were combined (trypsin, trypsin + chymotrypsin, and trypsin + Glu-C). As variable modifications, different oxidation products of cysteines (mono-, di-, trioxidation; *S*-thionylation as indicated, when samples were digested omitting reducing conditions) and methionines (mono- and dioxidation) were allowed. Lists of annotated MS2 spectra with a charge-dependent Xcorr score above the cutoff value (1.5, 2.0, 2.5, and 3.0 for 1+, 2+, 3+, and ≥4+ charge state, respectively) were exported to Excel and analyzed by the help of a pivot table. The number of MS2 spectra of each Met- or Cys-containing peptide and the corresponding methionine sulfoxide (Met-SO)- or Cys-ox–containing peptide was counted and calculated relative to their sum.

MsrA/MsrB Treatment of HypT. MsrA/MsrB treatment with purified HypT was performed using MsrA and MsrB (Jena Bioscience) at 1.2 μM each, 12 μM HypT-$HOCl^{2.75mM}$, and 12 mM DTT at 37 °C for 2 h. As control, 12 μM HypT-$HOCl^{2.75mM}$ was treated with 12 mM DTT alone (no MsrA/MsrB) or with MsrA/MsrB alone (no DTT) at 37 °C for 2 h. For fluorescence anisotropy, MsrA, MsrB, and DTT were removed by gel filtration (Superose 6; GE Healthcare). HypT-$HOCl^{2.75mM}$ before/after MsrA/MsrB treatment was analyzed by circular dichroism to ensure correctly folded protein.

Analysis of the Effect of MsrA/MsrB on HypT in Vivo—Protein Purification, Fluorescence Anisotropy, and MS Analysis. JC15 [BL21(DE3) pET11a-*hypT*] and AD29 [BL21(DE3) *msrA*$^-$ *msrB*$^-$ pET11a-*hypT*] cells were cultivated in 1.2 L LB medium until an OD of 0.45 was reached. Then, HOCl was added (2.75 mM final concentration), cultures were mixed, and the cells were centrifuged (6,500 rpm, 5 min, 4 °C) (total time of stress, 10 min). The cell pellet from 400 mL cells was resuspended in buffer (50 mM Tris·HCl, pH 7.5, 300 mM NaCl, 10 mM imidazole) and stored at −80 °C. For recovery, the cell pellet from 800 mL cells was resuspended in fresh LB medium containing 50 μg/mL tetracycline and further incubated at 25 °C. Samples were removed after 10 and 25 min, centrifuged (6,500 rpm, 5 min, 4 °C), resuspended in buffer, and stored at −80 °C (total recovery time, 15 and 30 min, respectively). Please note that, due to the large culture volumes required for purification, sample removal required more time than sample removal for qRT-PCR. For samples without quenching, HOCl was added to cells and samples were removed after 5, 20, and 35 min (total time of stress, 10, 25, and 40 min, respectively, corresponding to the time points for quenched samples; see above). Protein was purified as described above and used for fluorescence anisotropy and MS analysis.

Analytical Ultracentrifugation. Analytical ultracentrifugation was performed exactly as described (3).

Analysis of Intracellular Unincorporated Iron. Electron paramagnetic resonance spectrometry analysis was performed exactly as described (3).

HypT Secondary Structure Prediction and Structural Model. Secondary structure prediction of HypT was performed using the secondary prediction software Phyre 2 (4). The alignment of the HypT and *Escherichia coli* oxidative stress regulator OxyR sequences was performed using the program T-Coffee (5). The HypT structure was modeled using the structure prediction software Phyre 2 and then overlaid with the structure of reduced *E. coli* OxyR [Protein Data Bank (PDB) ID code 1I69 (6)]. It should be noted that the structure shown for HypT is only a model.

1. Datsenko KA, Wanner BL (2000) One-step inactivation of chromosomal genes in *Escherichia coli* K-12 using PCR products. *Proc Natl Acad Sci USA* 97(12):6640–6645.
2. Winter J, Linke K, Jatzek A, Jakob U (2005) Severe oxidative stress causes inactivation of DnaK and activation of the redox-regulated chaperone Hsp33. *Mol Cell* 17(3):381–392.
3. Gebendorfer KM, et al. (2012) Identification of a hypochlorite-specific transcription factor from *Escherichia coli*. *J Biol Chem* 287(9):6892–6903.
4. Kelley LA, Sternberg MJ (2009) Protein structure prediction on the Web: A case study using the Phyre server. *Nat Protoc* 4(3):363–371.
5. Notredame C, Higgins DG, Heringa J (2000) T-Coffee: A novel method for fast and accurate multiple sequence alignment. *J Mol Biol* 302(1):205–217.
6. Choi H, et al. (2001) Structural basis of the redox switch in the OxyR transcription factor. *Cell* 105(1):103–113.

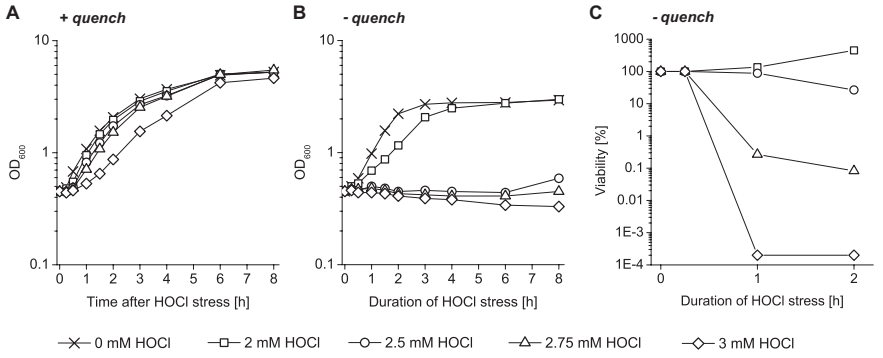

Fig. S1. Analysis of the effect of HOCl on the growth and viability of *E. coli* C600. C600 cells were cultivated in LB medium until OD_{600} 0.45–0.5 and then split; 10 mL was distributed to fresh flasks and HOCl was added (final concentration: 2, 2.5, 2.75, 3 mM) or cells were left unstressed as a control. After 10 min, (*A*) 2 mL of fivefold concentrated LB medium was added to stop the stress and allow recovery of cells and OD_{600} was followed (+quench), or (*B* and *C*) HOCl was not quenched (−quench) and then either (*B*) OD_{600} was followed or (*C*) viability was analyzed.

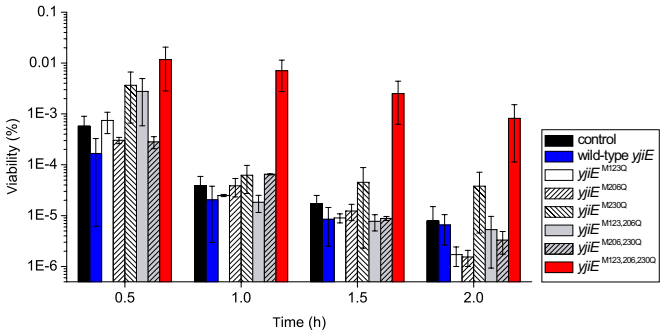

Fig. S2. Analysis of the contribution of methionine residues to HypT activity. Viability assay of C600 *recA*$^{-}$ *hypT*$^{-}$ cells (RecA is a DNA strand exchange and recombination protein) carrying an empty plasmid (control) or expressing wild-type *hypT*; single mutants *hypT*^{M123Q}, *hypT*^{M206Q}, and *hypT*^{M230Q}; double mutants *hypT*^{M123,206Q} and *hypT*^{M,206,230Q}; and the triple mutant *hypT*^{M123,206,230Q} after treatment with 2 mM H_2O_2. Viability was analyzed at the indicated time points. Please note that the *recA*$^{-}$ strain is incapable of DNA repair and suffers from H_2O_2-derived DNA damage and concomitant reduced viability. Please also note that the substitution of three methionines by glutamine is required for constitutively increased viability of the *recA*$^{-}$ *hypT*$^{-}$ strain. Results are expressed as mean ± SD of three experiments.

A

Oxidized peptide containing:	Number of MS2 spectra: *msrA*$^+$ *msrB*$^+$ (Fig. 5*C*)			*msrA*$^-$ *msrB*$^-$ (Fig. 5*F*)			*in vitro* (Fig. 5*H*)		
	-HOCl	+HOCl	+HOCl 15 min recovery	-HOCl	+HOCl	+HOCl 15 min recovery	+DTT	+MsrA/MsrB	+MsrA/MsrB +DTT
Met1-SO	n=270	n=106	n=122	n=61	n=144	n=182	n=134	n=101	n=308
Met123-SO	n=14	n=7	n=13	n=5	n=51	n=65	n=7	n=31	n=42
Met230-SO	n=176	n=135	n=138	n=56	n=125	n=246	n=70	n=51	n=433
Met284-SO	n=48	n=19	n=14	n=10	n=18	n=21	n=11	n=5	n=48

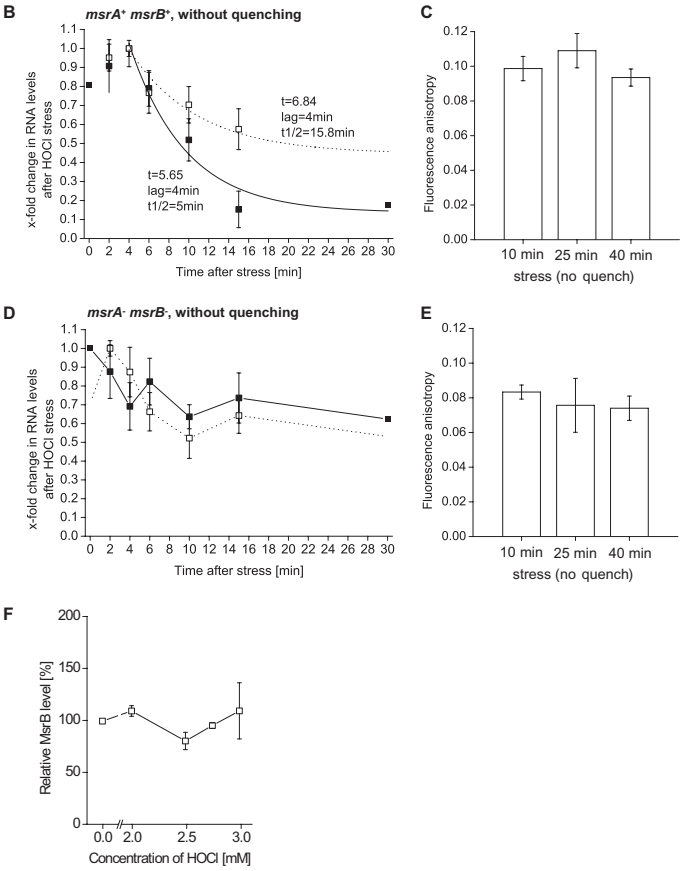

Fig. S3. HypT inactivation depends on MsrA/MsrB and quenching of HOCl. (*A*) Combined number of MS2 spectra of the respective methionine- and Met-SO–containing peptides from digested samples shown in Fig. 5 *C*, *F*, and *H*. (*B*–*E*) *E. coli msrA*$^+$ *msrB*$^+$ cells (*B* and *C*) and *msrA*$^-$ *msrB*$^-$ cells (*D* and *E*) were treated with HOCl (2.75 mM) and the HOCl was not quenched. Samples were removed at the indicated time points. (*B* and *D*) MetN RNA levels in stressed cells (*B*: C600 *msrA*$^+$ *msrB*$^+$ *hypT*$^-$; *D*: C600 *msrA*$^-$ *msrB*$^-$ *hypT*$^-$) either carrying an empty pBAD22 (control; closed symbol) or expressing *hypT* from pBAD22 (open symbol) by qRT-PCR. Shown are mean ± SD ($n = 3$). Shown are relative values; the highest value in one set of samples was set to 1. In *msrA*$^+$ *msrB*$^+$ cells (*B*), MetN RNA levels started decreasing after a lag time of 4 min. The time constant was $t = 5.65$ min and $t_{1/2} = 5$ min (control) and $t = 6.84$ min and $t_{1/2} = 15.8$ min (*hypT*-expressing cells). In *msrA*$^-$ *msrB*$^-$ cells (*D*), no reliable kinetic parameters for MetN RNA levels could be calculated because they remained above 50% of the stress level. (*C* and *E*) DNA binding of HypT purified from stressed BL21(DE3) cells (*C*: *msrA*$^+$ *msrB*$^+$; *E*: *msrA*$^-$ *msrB*$^-$) as determined by fluorescence anisotropy. Results are expressed as mean ± SD ($n = 3$). The time points correspond to the time points shown in Fig. 5 *B* and *E*. (*F*) Analysis of cellular MsrB levels in C600 cells. C600 cells were treated with the indicated HOCl concentrations, and samples were removed after 10 min and analyzed by Western blot using MsrB-specific antibodies. The intensity of MsrB bands was quantified using ImageJ software. Results are expressed as mean ± SD ($n = 3$).

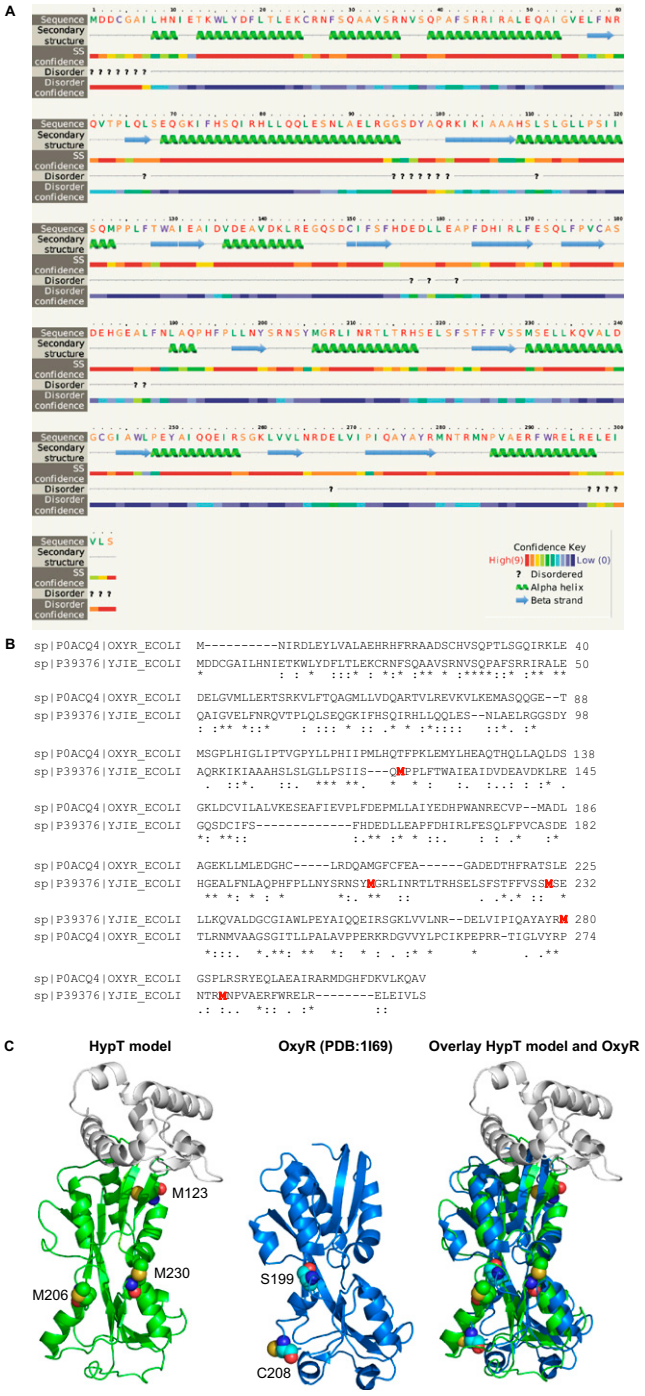

Fig. S4. HypT-predicted secondary structure and alignment with OxyR. (*A*) Secondary structure prediction of HypT using Phyre 2. (*B*) Alignment of the HypT and *E. coli* OxyR sequences using T-Coffee. The methionine residues in HypT are indicated in red. (*C*) (*Left*) The HypT structure was modeled using Phyre 2. Amino acids M123, M206, and M230 are shown as spheres. The N-terminal DNA-binding domain is shown in gray. (*Center*) The structure of reduced *E. coli* OxyR [PDB ID code 1I69 (6)]. Amino acids S199 (cysteine in wild-type OxyR) and C208 are shown as spheres. (*Right*) Overlay of the modeled HypT and the reduced OxyR structures.

Table S1. Strains used in this study

Strain name	Relevant genotype	Plasmid	Source
JC15	BL21(DE3) gold	pJC2 (pET11a-*hypT-His*)	(3)
JW469	BL21(DE3) gold *msrA*$^{-}$ *msrB*$^{-}$		This study
AD29	JW469	pJC2	This study
AD27	BL21(DE3) gold	pET11a-*hypT*^{M123,206,230Q}	This study
AD44	BL21(DE3) gold	pET11a-*hypT*^{M123,206,230,284Q}	This study
AD27	BL21(DE3) gold	pET11a-*hypT*^{M123,206,230I}	This study
C600	*thr leu thi lac4 rpsL supE* (F^{-})		*E. coli* Genetic Stock Center
KMG214	C600 *hypT*::Cm		(3)
Yle143	KMG214	pJW2	(3)
KMG229	KMG214	pJW2-*hypT*	(3)
YLe256	KMG214	pJW2-*hypT*^{M123Q}	This study
YLe228	KMG214	pJW2-*hypT*^{M206Q}	This study
YLe229	KMG214	pJW2-*hypT*^{M230Q}	This study
YLe258	KMG214	pJW2-*hypT*^{M280Q}	This study
YLe230	KMG214	pJW2-*hypT*^{M284Q}	This study
JW470	KMG214	pJW2-*hypT*^{M123I}	This study
YLe220	KMG214	pJW2-*hypT*^{M206I}	This study
YLe221	KMG214	pJW2-*hypT*^{M230I}	This study
YLe257	KMG214	pJW2-*hypT*^{M280I}	This study
YLe222	KMG214	pJW2-*hypT*^{M284I}	This study
AD56	KMG214	pJW2-*hypT*^{C4S}	This study
YLe231	KMG214	pJW2-*hypT*^{C25S}	This study
AD60	KMG214	pJW2-*hypT*^{C150S}	This study
YL232	KMG214	pJW2-*hypT*^{C178S}	This study
AD57	KMG214	pJW2-*hypT*^{C242S}	This study
JW458	KMG214	pJW2-*hypT*^{M123,206,230Q}	This study
JW477	KMG214	pJW2-*hypT*^{M123,206,230I}	This study
JW454	KMG214 *recA*::Km		This study
JW460	JW454	pJW2	This study
JW457	JW454	pJW2-*hypT*	This study
JW461	JW454	pJW2-*hypT*^{M123Q}	This study
JW462	JW454	pJW2-*hypT*^{M206Q}	This study
JW463	JW454	pJW2-*hypT*^{M230Q}	This study
JW464	JW454	pJW2-*hypT*^{M123,206Q}	This study
JW465	JW454	pJW2-*hypT*^{M206,230Q}	This study
JW459	JW454	pJW2-*hypT*^{M123,206,230Q}	This study
KMG232	KMG214, Cm cassette removed		This study
HM15	KMG232 *msrA*::Cm *msrB*::Km		This study
HM16	HM15	pJW2	This study
HM17	HM15	pJW2-*hypT*	This study